ARTICLE
Journal of Cellular Biochemistry 106:776–786 (2009)

Journal of Cellular Biochemistry

Proteomic Profiling of Distinct Clonal Populations of Bone Marrow Mesenchymal Stem Cells

Shobha Mareddy,[1] James Broadbent,[2] Ross Crawford,[1,3] and Yin Xiao[1*]

[1]*Medical Device Domain, Institute of Health and Biomedical Innovation, Queensland University of Technology, 60 Musk Ave., Kelvin Grove, Brisbane, QLD 4059, Australia*

[2]*Cells and Tissue Domain, Institute of Health and Biomedical Innovation, Queensland University of Technology, 60 Musk Ave., Kelvin Grove, Brisbane, QLD 4059, Australia*

[3]*Prince Charles Hospital, Orthopaedic Surgery, Rode Road, Chermside, QLD 4032, Australia*

ABSTRACT

Mesenchymal stem cells (MSCs) have attracted immense research interest in the field of regenerative medicine due to their ability to be cultured for successive passages and multi-lineage differentiation. The molecular mechanisms governing MSC self-renewal and differentiation remain largely unknown. The development of sophisticated techniques, in particular clinical proteomics, has enabled researchers in various fields to identify and characterize cell specific biomarkers for therapeutic purposes. This study seeks to understand the cellular and sub-cellular processes responsible for the existence of stem cell populations in bone marrow samples by revealing the whole cell proteome of the clonal cultures of bone marrow-derived MSCs (BMSCs). Protein profiling of the MSC clonal populations was conducted by Two-Dimensional Liquid Chromatography/Matrix-Assisted Laser Desorption/Ionisation (MALDI) Mass Spectrometry (MS). A total of 83 proteins were identified with high confidence of which 11 showed differential expression between subpopulations, which included cytoskeletal and structural proteins, calcium binding proteins, cytokinetic proteins, and members of the intermediate filament family. This study generated a proteome reference map of BMSCs from the clonal populations, which will be valuable to better understand the underlying mechanism of BMSC self-renewal and differentiation. J. Cell. Biochem. 106: 776–786, 2009.

KEY WORDS: MESENCHYMAL STEM CELLS; PROTEOMICS; CLONAL POPULATIONS; BONE MARROW STROMAL CELLS

Bone marrow-derived mesenchymal stem cells (BMSCs) offer an attractive source of adult mesenchymal stem cells (MSCs) for the purpose of tissue regeneration. The versatility and availability of these cells make them a potent resource for cell transplant therapies. Although the potential use of BMSCs in therapeutic applications is well documented, unlike haematopoietic stem cells, BMSCs are less characterized and knowledge of their underlying molecular and cellular events remains unclear.

Previous studies suggest human BMSC populations, in vitro and in vivo, are morphologically and functionally heterogeneous. Several attempts have been made to identify cell surface markers for the purification of stem cells from the mixed BMSC populations. A panel of cell surface markers have been investigated in the MSC separation such as STRO-1, CD29, CD44, CD73, CD90, CD105, CD166, and MHC-1 [Simmons et al., 1991; Gronthos et al., 2003; Kolf et al., 2007]. However, all these putative mesenchymal markers are not uniquely expressed in stem cells and the quest to find typical markers that determine the fate and function of mesenchymal stem cells still remains active.

In our previous study we focused on developing single-cell clones derived from BMSCs and investigated their clonal characteristics [Mareddy et al., 2007]. Altogether, 14 clonal populations were established from three bone marrow stromal samples. The clones were grouped into fast-growing clones and slow-growing clones based on their proliferative capacities, which was to measure the time taken by the individual clones to reach 20 population doubling. Upon differentiation five of six fast-growing clones were capable of differentiating towards osteogenic, chondrogenic and adipogenic lineages. However, the slow-growing clones showed limited differentiation potential and morphological changes associated with cellular senescence with extended duration in culture. Flow cytometric analysis found no obvious difference in the expression of the selected characteristic BMSC cell surface markers CD29, CD44, CD90, CD105, and CD166 between fast-growing and slow-growing

*Correspondence to: Associate Prof. Yin Xiao, Institute of Health and Biomedical Innovation, Queensland, University of Technology, Kelvin Grove Campus, Brisbane, QLD 4059, Australia. E-mail: yin.xiao@qut.edu.au

Received 9 October 2008; Accepted 8 January 2009 • DOI 10.1002/jcb.22088 • 2009 Wiley-Liss, Inc.
Published online 19 February 2009 in Wiley InterScience (www.interscience.wiley.com).

clones [Mareddy et al., 2007]. To understand the molecular mechanisms governing MSC self-renewal and differentiation, three fast-growing clones with tripotential differentiation capacity (designated stem cell clones (SCCs)) and three slow-growing clones with only unipotential differentiation capacity (designated non-stem cell clones (nSCCs)) were selected for this study to investigate the proteomic profiling of these distinct clonal populations.

Proteomics is the study of protein complement and aims to identify and characterize the entire protein make up of a sample, whether originating from a cell, tissue type or whole organism. A comparative approach to proteomics allows for the discovery of potential biomarkers or therapeutic targets that exist at a functional level in the cell by highlighting protein differences between test and control samples [Lane, 2005]. Although proteomic analysis of human mesenchymal stem cells have been conducted previously [Foster et al., 2005; Salasznyk et al., 2005; Park et al., 2007], the comparison of proteomic profiles from distinct cell populations derived from clone culture of bone marrow samples has the potential to reveal proteins that are important to the differences observed between these populations.

MATERIALS AND METHODS

CLONE CULTURE AND CHARACTERIZATION OF BMSCs

Protein profiling studies were conducted on the previously characterized SCCs (fast-growing with tripotential differentiation capacity) and nSCCs (slow-growing with unipotential differentiation capacity) derived from BMSCs as described in our previous study [Mareddy et al., 2007]. Three SCC and three nSCC clones were selected from three different BMSC sample. To narrow down the variations, each BMSC sample contained one SCC and one nSCC clone respectively. Bone marrow samples were obtained from osteoarthritis patients aged from 54 to 76 (two females and three males) under elective knee replacement surgery. Patients selected for this study stopped all anti-inflammatory medicine 10 days prior to the surgery. Great care was taken to avoid contamination with MSC from other sources. The source of bone marrow in the present study was from the femoral canal. As per the standard knee replacement operation procedure, the joint was opened followed by draining of synovial fluid and extensive lavage. A femoral drill hole was made through the distal femur and an intramedullary rod was passed into the femoral canal. The marrow that oozed out was aspirated by a syringe. Single-cell clone cultures were established by a limiting dilution method. The number of viable cells/ml was determined at each passage using a haemocytometer. A graph was plotted against time in culture for a single cell to reach a population of approximately 1 million cells, or to undergo 20 population doublings (PDs), to measure the proliferative ability. A visual examination of cell proliferation between SCCs and nSCCs was conducted by plating cells at 8th passage at a density of 8,000 cells per well in a 24-well plate. After 3 days in culture the cells were fixed with 4% paraformaldehyde for 15 min and stained with crystal violet for 10 min. Excess stain was washed away with tap water and after drying the plates were examined by microscopy.

The expression of surface antigens against CD29, CD34, CD45, CD44, CD73, CD90, CD105, CD166, and major histocompatibility complex (MHC class I, and MHC class II) was characterized by fluorescent flow cytometry (FACS) using cells at sixth passage. Briefly, confluent cultures were harvested in 0.05% trypsin/EDTA for 1 min and pelleted at 1,000 rpm for 10 min. Cells were re-suspended in FACS buffer (PBS + 0.1% (w/v) sodium azide + 1% (w/v) bovine serum albumin) and incubated with primary unconjugated antibodies (CD29, CD34, CD45, CD44, CD73, CD90, CD105, CD166), major histocompatibility complex (MHC class I, and MHC class II) (BD Biosciences, Clontech, Palo Alto, CA) for 15 min at room temperature. The cells were then washed and incubated with secondary antibody (goat anti-mouse immunoglobulin G phycoerythrin conjugate, Jackson Immunoresearch Laboratories, West Grove, PA) for 15 min. The cells were then washed and analysed using flow cytometry on a FACS Calibur (Becton Dickinson, Cowley, Oxford, UK). Data was analysed using FCSExpress™ software.

PROTEOMIC ANALYSIS

Preparation of cell lysis buffer. The lysis buffer consisted of 7.5 M urea, 2.5 M thiourea, 12.5% glycerol, 62.5 mM Tris–HCl 2.5% (w/v) n-octylglucoside (octyl α-D-glucopyranoside), 6.25 mM TCEP (Tris (2-carboxyethyl) phosphine hydrochloride), 1.25 mM protease inhibitor cocktail containing 4-(2-aminoethyl)benzenesulfonyl fluoride (AEBSF), E-64, bestatin, leupeptin, aprotinin, and sodium EDTA. Stock Lysis Buffer was prepared according to the ProteomeLab™ PF 2D manufacturer's protocol (Beckman Coulter, Fullerton, CA). All the above chemicals were biotechnology grade from Sigma Aldrich Pty (Castle Hill, New South Wales, Australia).

Sample preparation. All SCC or nSCC clones were pooled for protein extraction. SCCs and nSSCs at passage 8 were plated at a density of 5×10^3 cells/cm^2 in a 175 cm^2 flask were cultured in Dulbecco's modified Eagle medium with low glucose (DMEM-LG) (GIBCO, Invitrogen Corporation, Australia) supplemented with batch tested 10% (v/v) foetal bovine serum (FBS) and 5% 10 U/ml penicillin G and 10 μg/ml streptomycin (GIBCO). The cells were incubated at 37°C in a humidified condition containing 5% CO_2. Eight flask cells from SCCs or nSCCs were pooled together and washed twice in Dulbecco's phosphate buffered saline, DPBS (GIBCO). A total volume of 500 μl of the cell pellet was suspended in 2 ml of lysis buffer containing 1.25 mM protease inhibitor cocktail and vortexed rigorously. The suspension was centrifuged at 20,000g for 60 min at 18°C. The resulting supernatant was stored at −80°C until further use. Protein concentration was determined with a BCA™ protein assay kit (Pierce, Quantum Scientific, QLD, Australia) on the sample lysate after exchange with Start Buffer on a PD-10 size exclusion column (GE Healthcare Biosciences, NSW, Australia).

1st-Dimension separation—chromatofocusing. First and second dimension separations were based on the ProteomeLab™ PF 2D default method [Betgovargez et al., 2005]. Start and Eluent Buffers, supplied in the PF 2D chemistry kit (Beckman Coulter), were sonicated for 5 min and pH adjusted to 8.5 ± 0.1 and 4.0 ± 0.1 with saturated iminodiacetic acid (Sigma) and 1 M NH_4OH accordingly. Chromatofocusing was performed at ambient temperature with a flow rate of 0.2 ml/min, and absorbance of the column effluent was monitored at 280 nm. The chromatofocusing column was first

equilibrated with 30 volumes of Start Buffer, after which 3.2 mg of protein sample, previously exchanged into Start Buffer, was injected onto the column. Proteins were then fractionated by their isoelectric point (pI) over a chromatographic pH gradient of pH 8.5 to 4.0. Liquid fractions were collected at 0.3 pH intervals during the pH gradient and at 5 min intervals at all other times. The first dimension fractions were collected into a 96-well plate by the combination fraction collector/auto-injector (FC/I).

2nd-Dimension separation—high performance reversed-phase chromatography. The pI fractions from the first dimension were sequentially injected onto the second dimension high performance reverse phase liquid chromatography column as specified in the ProteomeLab™ PF 2D user manual. The first dimension fractions were separated based on their hydrophobicity over a solvent gradient of H_2O/0.1% Triflouroacetic acid (TFA), (Solvent A) and acetonitrile/0.08% TFA, (Solvent B). HPLC grade acetonitrile and TFA were purchased from Sigma Aldrich Pty (NSW, Australia). The second dimension separation was performed at 50°C at a flow rate of 0.75 ml/min and column eluent absorbance was measured at 214 nm. The column was first equilibrated with 10 volumes of 100% Solvent A. From each first dimension fraction 200 µl was injected and the column was eluted with a gradient of 0–100% Solvent B. The reversed phase fractions were collected at a rate of 1 min/fraction into 96-deep well plates for subsequent processing and digestion with trypsin for analysis by mass spectroscopy, without any additional extraction or solubilization of the sample with other fractionation techniques.

Data analysis. UV absorbance profiles, appearing similar to 2-D gels, were generated for each of the SCCs (fast-growing) and nSCCs (slow-growing) separations using the ProteoVue application of the ProteomeLab™ PF 2D Software Suite 1.0. A comparison of the UV absorbance profiles for SCCs and nSCCs was performed using the DeltaVue application of the software suite. The peak picking analytical tool of the DeltaVue software enabled semi-quantitation of differences in UV absorbance between the clone profiles and the results were displayed as fold changes.

Sample preparation and mass spectrometry. Selected reversed phase fractions were concentrated using a Speed Vac concentrator (Thermo Savant) and subsequently reduced by treating each fraction with 100 µl 0.1 M NH_4CO_3, pH 7.9, and 20 mM DTT (Sigma Aldrich) and incubated for 1 h at 56°C. Samples were then alkylated by adding 0.5 M iodoacetamide stock (Sigma Aldrich) for a final concentration of 50 mM in each tube and incubated for 30 min at 37°C in the dark. All the samples were digested with sequencing grade modified trypsin (Promega, NSW, Australia), by adding 0.1 µg/µl stock to a final concentration of 2 ng/µl and incubated overnight at 37°C. The tryptic peptides were then desalted using PerfectPure C-18 tips (Eppendorf, Quantum Scientific, Brisbane, Australia) and 0.4 µl of each sample was applied to a MALDI target plate (96 × 2 spot ABi 4700 target), which had been spotted just prior with 0.4 µl of α-cyano-4-hydroxy-trans-cinnamic acid (CHCA) matrix (Sigma) at a concentration of 5 mg/ml in 60% acetonitrile, 0.1% TFA. The spots were air dried and MALDI-TOF/TOF-MS analysis was performed using a 4700 Proteomics Analyser mass spectrometer (Applied Biosystems) operated in positive ion reflectron mode. MS data were calibrated using a plate wide external calibration using the 4700 Mass Standards Kit (Applied Biosystems) containing des-Arg-Bradykinin (MH+ 904.458) Angiotensin I (MH+ 1296.685) Glu-fibrinopeptide B (MH+ 1570.677) ACTH (1–17 clip, MH+ 2093.087), ACTH (18–39 clip, MH+ 2465.199) and ACTH (7–38 clip, MH+ 3657.929). MS/MS data were calibrated against the MS/MS fragments of the $m/z = 1296.685$ Angiotensin I peptide in the standards. MS data was acquired using 2000 shots. The top 10 most intense peptides detected in each spot in MS mode were automatically selected for MS/MS analysis using 3000 laser shots.

Peptide identification. The MASCOT (Matrix Science) search engine was used to deconvolute the raw mass spectra to obtain a list of probability-based protein/peptide matches for each of the samples. The MSDB database was selected and taxonomy restricted to *Homo sapien*; trypsin cleavage specificity was allowed one missed cleavage, peptide tolerance was limited to 50 ppm, modifications were set to carbamidomethylation of cysteine (fixed), and oxidation of methionine (variable).

WESTERN BLOT ANALYSIS

Three SCC and nSCC samples were validated by the protein expression. Total protein lysate (5 µg) from SCCs and nSCCs cultures at passage 8, were separated by sodium dodecyl sulfate–polyacrylamide gel electrophoresis (SDS–PAGE) and transferred to a nitrocellulose membrane. The blots were blocked with Tris-buffered saline containing 0.1% Tween-20 and 5% non-fat milk, followed by incubation with primary antibodies against calmodulin (CAM) (mouse anti-human, Millipore, NSW, Australia), heat shock protein 27 (HSP27) (rabbit anti-human, Bio Scientific Pty, NSW, Australia) and alpha tubulin (TUB) (mouse anti-human, Abcam, Sapphire Bioscience, NSW, Australia) at 1:1,000 dilution. The bound primary antibodies were detected by using a goat anti-mouse for CAM and TUB and goat anti-rabbit IgG-horseradish peroxidase conjugated antibody for HSP27 (1:1,000) and bands were visualized by electrogenerated chemiluminescence (ECL). Band intensity of CAM and HSP27 was measured and normalised via the expression of TUB.

IMMUNOCYTOCHEMISTRY

Clonal cultures at passage 9 were plated at a density of 3,000 cells/well on 8-well chamber slides (Uunc, In Vitro Technologies Pty Ltd, Victoria). The cells were allowed to attach overnight at 37°C in a CO_2 incubator, and fixed in 4% paraformaldehyde in phosphate-buffered saline (PBS) for 15 min, followed by permeabilization with 0.5% triton X-100 in PBS for 10 min. Non-specific protein binding was blocked by incubation with 1:10 normal swine serum in PBS containing 0.1% bovine serum albumin (BSA) for 30 min. The cells were immunostained against CAM, HSP27 and TUB (positive control) by incubating with a 1:1,000 primary antibody dilution in PBS with 0.1% BSA at 4°C overnight. Cells were then incubated with a biotinylated swine-anti-mouse, rabbit, goat antibody (DAKO Multilink, CA) for 15 min, and then incubated with horseradish perioxidase-conjugated avidin-biotin complex (ABC) for 15 min. Antibody complexes were visualized after the addition of a buffered diaminobenzidine (DAB) substrate for 4 min. The reaction was stopped by immersion and rinsing of sections in PBS. Cells were then

lightly counterstained with Mayer's haematoxylin and Scott's Blue for 40 s each, in between 3 min rinses with running tap water. Following this, the cells were dehydrated with ascending concentrations of ethanol solutions, cleared with xylene and mounted with a cover slip using DePeX mounting medium (BDH Laboratory Supplies, England). Control for the immunocytochemical cell staining procedures included conditions where the primary antibody was omitted.

QUANTITATIVE RT-PCR (QRT-PCR)

Total RNA was isolated from SCCs and nSCCs cultures at passage 9 using Tri Reagent (Sigma) following the suppliers instructions. RNA concentration was measured by photometric measurement. Total RNA (1 μg) was reverse transcribed into 20 μl cDNA using SuperScript III (Invitrogen) following the manufacturers protocol. Real-time PCR was performed in 25 μl reactions containing 12.5 μl SYBR green Master Mix (Applied Biosystems), 2.5 μl (10 μM) of each forward and reverse primer for each gene of interest for a final concentration of 20 pmol, 2.5 μl of cDNA template and RNA free water. Reactions were performed in triplicates to determine the expression of genes using primers (Table I) for CAM, HSP27, and CAD. The house keeping gene, 18S rRNA was used as a control. The reaction was carried out using ABi Prism 7000 Sequence Detection System (Applied Biosystems) and the PCR amplification followed 1 cycle of 30 min at 48°C, 1 cycle of 10 min at 95°C, 40 cycles of 15 s at 95 and 60°C for 1 min. Melting curve analysis was performed to validate specific amplicon amplification without genomic DNA contamination. Relative expression levels for each gene were normalized by the Ct value of the house keeping gene 18S rRNA and determined by using the ΔCt method. The genes for CAM, HSP27 and CAD were selected for real time-PCR analysis due to their high relevance to cell integrity and confident mass spectrometry identifications. The relative expression of each gene was analysed by one-way ANOVA and Student–Newman–Keuls (SNK) q-test. The significant difference was considered at $P < 0.05$.

RESULTS

In our previous study SCCs have been demonstrated to be able to differentiate to osteogenic, chondrogenic and adipogenic lineages, whereas nSCCs showed limited differentiation [Mareddy et al., 2007]. In this study three SCCs and three nSCCs clones were selected to further compare their growth kinetics. At 8th passage, SCCs clones demonstrated fast-growing ability after plating in tissue culture well for 3 days compared with nSCCs (Fig. 1A). The time for SCCs to reach 20 PDs was significantly shorter than nSCCs ($P = 0.0116$) (Fig. 1B). FACS analysis revealed that all the clones were positive for mesenchymal cell surface epitopes (CD29, CD44, CD73, CD90, CD105, and CD166) and negative for haematopoietic cell surface epitopes (CD34 and CD45). Furthermore, all the clones expressed MHC class I but were negative for MHC class II. There was no significant difference between the two types of clones in the expression of these cell surface markers ($P > 0.05$) (Fig. 1C).

DIFFERENTIAL PROTEIN EXPRESSION PROFILE OF CLONAL POPULATIONS

Pooled proteins from SCC and nSCC samples were used for the study of protein expression profile of SCCs and nSCCs. Two dimensional proteomic profiles of the pooled SCC (Fig. 2A) and nSCC (Fig. 2B) samples were obtained from 2D-LC fractionation. Identifiers located on the proteome maps indicate identified proteins (see below). Each lane represents the UV absorbance (214 nm) intensity of the reversed-phase high-performance chromatography separation for each fraction collected in the chromatofocusing separation. The pI window for each fraction is detailed at the top of each lane and the reversed-phase retention time is detailed at the left. The fractions resulting from reversed phase separation of SCCs and nSCCs exhibited differences in the expression of proteins in the order of fold changes ranging from 1 to 5. Based on these fold differences, fractions with a fold change greater than 1.5 were selected for further analysis with MALDI-TOF/TOF-MS. The identity of the resulting proteins were then determined by comparing the masses obtained by MS and MS/MS analysis to the theoretical masses of in silico digested proteins using a MASCOT (Matrix Science Ltd.) database search.

The MS results depicted a high abundance of proteins belonging to the intermediate filament family, cytoskeletal components, calcium-binding proteins and metabolic enzymes. Essentially the proteins which showed a MOWSE (molecular weight search) protein score above 64 were further ranked by peptide fragmentation mass fingerprint (PFMF) scores when considering protein identification. The proteins calmodulin (CAM) and heat shock protein 27 (HSP27) were unequivocally identified by PFMF. A total of 83 proteins representing 196 second-dimension liquid fractions were identified in this study (Table II). The location of identified proteins on proteome reference maps can be observed in Figure 2 using the identification numbers in column 1 of Table II. The molecular function and biological processes of these proteins were assigned according to information found in the Swiss-Prot and NCBI protein databases. A group of six proteins were expressed repeatedly in more than one non-sequential fraction, suggesting these proteins may have undergone post-translational modification. Altogether, 11 proteins of specific interest were identified by MS, with high protein and ion score intervals, which were differentially expressed between

TABLE I. Primer Pairs Used in qRT-PCR Analysis

Gene	Abbreviation	Forward primer	Reverse primer
Calmodulin	CAM	5′-TTGACAAGGATGGCAATGGTTATA-3′	5′-GACTTGTCCGTCTCCATCAATATCT-3′
Caldesmon	CAD	5′-CTGCTGAAGGTGTACGCAACA-3′	5′-AAGCCAGCAGTTTCCTTATTTGG-3′
Heat shock protein 27	HSP27	5′-TCCCTGGATGTCAACCACTTC-3′	5′-TCGTGCTTGCCGGTGAT-3′
18S RNA	18S	5′-TTCGGAACTGAGGCCATGAT-3′	5′-CGAACCTCCGACTTCGTTC-3′

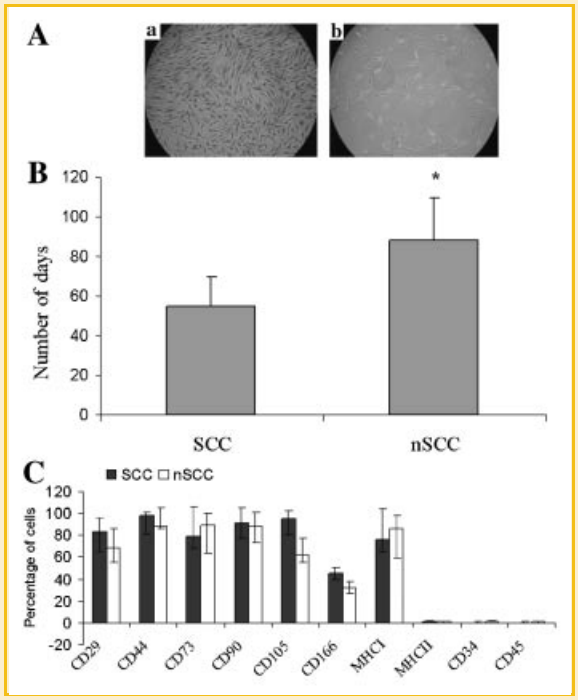

Fig. 1. Growth and surface marker characterization of SCCs. A: Morphologically no significant difference was noted between SCCs (a) and nSCCs (b), but increased cell number was visually observed in SCCs compared with nSCCs after 3 days in culture with the same seeding density (10× magnifications). B: The chart indicates the time taken by SCCs and nSCCs ($n=3$) to complete 20 population doublings (PDs). SCCs reached a population of one million cells (approximately 20 PDs) within 55 days whereas nSCCs took more than 88 days ($P=0.018$). C: Flow cytometry analysis of surface epitopes in bone marrow derived clone cultures. Clone cultures were labeled with phycoerythrin or fluorescein isothiocyanate-conjugated antibodies against putative mesenchymal (CD29, CD44, CD73, CD90, CD105, CD166), haematopoietic (CD34 and CD45), major histocompatibility complex (MHCI and MHCII) and immunoglobulin (Ig) isotope controls. The chart shows that there was no significant difference in the expression of these surface markers between SCCs and nSCCs. Error bars reflect the mean (±SD) across 3 SCCs and 3 nSCCs.

SCCs and nSCCs (Table III). Among them, three were up-regulated in SCCs and 8 up-regulated in nSCCs. These proteins included cytoskeletal, cytokinetic, stress related proteins and proteins of energy and signalling pathways.

FUNCTIONAL GROUPING

In the list (Table II) of protein species identified, 52% are involved in biological processes such as cellular organization, which included cytoskeletal and structural, calcium binding proteins, cytokinetic and members of intermediate filament family. Other proteins identified were membrane proteins (11%), metabolic enzymes (13%), endocrine proteins (7%), transport proteins (2%), stress proteins (2%), and some unknown proteins (13%).

The three most frequently observed proteins in SCCs were calmodulin (CAM) and tropomyosin (TM), which are intermediate filament proteins and corticotropin secreted by the pituitary gland (Table III). The eight most abundant proteins in nSCCs were caldesmon (CAD), annexin 1, lamin A/C, progerin, metabolic pathway enzymes, glyceraldehyde-3-phosphate dehydrogenase (GAPDH), enolase and pyruvate kinase M2 and a stress related protein, HSP27 (Table III). Vimentin, a structural protein was found abundantly in both groups of clones.

CONFIRMATION STUDIES

Proteomics findings were evaluated in SCC and nSCC clonal populations derived from original sample, as well as two additional patient samples. Results were validated by the mRNA expression using quantitative PCR for CAM, CAD, and HSP27; protein expression using western blot analysis and immunocytochemical cell staining for the proteins CAM and HSP27. The mRNA and protein results were analogous to the protein presentation observed in proteomic study when comparing the clonal populations. The mRNA expression of CAM was significantly upregulated in SCCs compared to nSCCs; whereas mRNA expression of CAD and HSP27 was significantly downregulated in SCCs (Fig. 3A). Western blot analysis results showed CAM was highly expressed in SCCs (Mean intensity: 0.67, SD: 0.12) compared with the expression in nSCCs (Mean intensity: 0.41, SD: 0.09), whereas HSP27 was expressed more in nSCCs (Mean intensity: 0.71; SD: 0.2) and SCCs (Mean intensity 0.35; SD: 0.20) (Fig. 3B). Immunocytochemical staining of CAM and HSP27 further demonstrated the distribution of CAM in SCCs and HSP27 in nSCCs. Tubulin, which was used as a control was distributed equally in both SCCs and nSCCs. No staining was detected in the negative control (Fig. 4).

DISCUSSION

Cell based therapies rely to a large degree on the preparation of an effective dose of ex vivo expanded cells capable of self-renewal and differentiation. Identifying cells of physiological relevance forms an integral part of the emerging field of tissue engineering. During the past decade there has been an increase in research activity aimed at understanding cellular and molecular aspects of cell proliferation and differentiation of various sources of stem cells [Golan-Mashiach et al., 2005; Hermansson et al., 2004; Panepucci et al., 2004; Wang et al., 2004; Feldmann et al., 2005; Blonder et al., 2006]. Irrespective of stem cell source, cell quality for in vitro expansion is defined by certain desirable parameters. Cell proliferation rates need to be high in order to reach a sufficient quantity of cells for practical transplantation that can readily differentiate upon induction. A large volume of research has focused on finding subpopulations of cells which meet these criteria and then to identify specific markers which could enable isolation of such cells. A growing body of research indicates a need for, but a lack of, rigorous standards for characterizing human MSCs, and thus makes it difficult to compare data from different investigators [Phinney et al., 1999; Banfi et al., 2000; Muraglia et al., 2000]. Fewer studies have focused on protein expression profiles of the differentiation pathways of MSCs [Hermansson et al., 2004; Blonder et al., 2006; Sun et al., 2006; Ye et al., 2006]. Sun et al. [2006] conducted proteome analysis on serially subcultured MSCs during osteogenic differentiation from heterogeneous starting populations. They concluded that proteomic

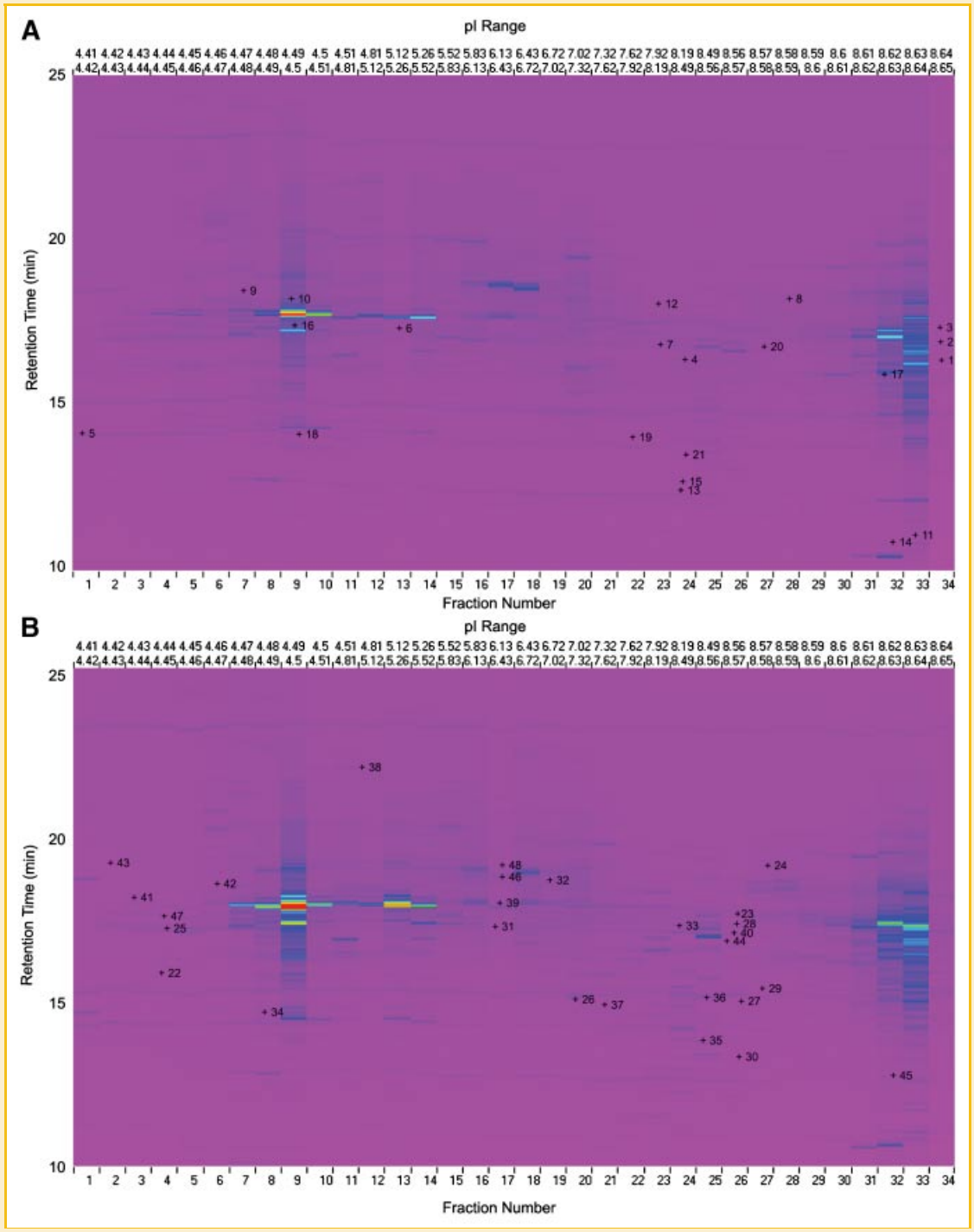

Fig. 2. Two dimensional proteomic profiles of the pooled SCC (A) and nSCC (B) samples obtained from 2D-LC fractionation. Each lane represents the UV absorbance (214 nm) intensity of the reversed-phase high-performance chromatography separation for each fraction collected in the chromatofocusing separation. The pI window for each fraction is detailed at the top of each lane and the reversed-phase retention time is detailed at the left. Crosshairs (+) designate proteins which were found to have differential presentation and were subsequently identified by mass spectrometry (see Table II). [Color figure can be viewed in the online issue, which is available at www.interscience.wiley.com.]

studies should ideally be conducted on colonies derived from a single cell origin, although such a procedure faces the limitation of cell number/quantity [Sun et al., 2006]. To our knowledge no proteomic studies have been conducted on the sub-populations derived from the heterogeneous bone marrow stromal cells. Our study is based on populations derived from single cells and which can therefore be assumed to be genetically homogenous, at least to begin with. To make up for the low quantity of cells, clonal populations were serially cultured up to 28 population doublings. No cytogenetic abnormalities were detected in all clonal populations

TABLE II. Identified Protein Expression Profile of SCC and nSCC Separated by 2D LC and Identified by MALDI-TOF/TOF-MS

ID # from Figure 2	Protein identification	Accession number	Protein molecular weight (Da)	MOWSE score (PS)	Protein Score confidence interval	No. of matched peptides	pI	Sequence coverage (%)	Fold changes
SCC									SCC/nSCC
1	Myomesin-1 (190K human protein)	P52179	163,719.6	67	96.972	10	6.1	8	4.828
2	AB208934 NID	BAD92171	139,599.9	73	99.185	10	7.75	11	3.718
3	AF126782 NID	AAF06941	32,589	63	92.737	6	9.05	9	3.678
4	Hypothetical protein FLJ35808 (fragment)	Q24KJ5	6,737.6	62	91.065	4	10.46	21	3.604
5	Corticotrophin-lipotropin (fragment)	P68000	4,538.3	79	98.411	1	8.09	56	3.44
5	ACTH (fragment)	CAA00890	4,692.3	69	98.297	1	8.34	53	3.44
5	Protein sequence 9 from patent number DE3731875	E972644	4,763.4	69	98.258	1	8.39	17	3.42
5	Hypothetical protein FLJ35808 (fragment)	Q24KJ5	6,737.6	62	91.065	4	10.46	21	3.42
6	AX886624 NID	CAF00762	6,869.5	66	96.009	4	11.71	16	3.401
7	KLHL5 protein (fragment)	Q6PD75	38,774.2	62	90.644	5	8.64	12	3.256
n/a	AB208934 NID	BAD92171	139,599.9	69	98.045	10	7.75	11	3.065
8	Tropomyosin	S05585	26,617.5	64	93.819	6	4.77	17	3.04
9	AX886624 NID	CAF00762	6,869.5	68	97.363	4	11.71	11	3.04
10	Vimentin—homo sapiens (human)	Q5JVT0	49,680.1	210	100	7	5.19	25	2.961
n/a	Hypothetical protein LOC130940 (fragment)	Q4ZG23	43,808.3	72	99.02	6	7.29	19	2.892
11	Myeloid/lymphoid or mixed-lineage leukemia	Q5TIH0	28,658.6	60	85.172	5	8.97	17	2.819
12	Nebulin, skeletal muscle	S55024	775,749.4	60	85.172	14	9.1	21	2.683
n/a	AY157850 NID	AAO16497	43,545.2	70	98.551	5	7.23	16	2.64
13	Hypothetical protein KIAA0465	T00079	194,733.5	67	97.302	10	6.84	18	2.62
14	Microtubule-actin crosslinking factor 1 (fragment)	Q5TBD2	508,010.3	64	94.362	13	5.22	3	2.286
15	Centriole associated protein CEP110	Q9Y489	117,425.5	63	92.218	8	5.43	16	2.247
16	Myeloid/lymphoid or mixed-lineage leukemia	Q5TIH0	28,658.6	60	85.172	5	8.97	17	2.245
17	Calmodulin—duck	P62144	16,838	104	100	4	4.09	45	2.235
17	Calmodulin, chain A	1CDLA	16,069.5	94	99.994	3	4.06	45	2.232
17	Tropomyosin alpha-4 chain	TPM4	28,487.5	89	99.981	4	4.67	17	2.15
18	Corticotropin—sei whale	PN0127	4,538.3	79	99.805	1	8.09	53	2.114
19	ACTH (fragment)	CAA00890	4,692.3	79	99.795	1	8.34	53	2.108
20	Vimentin	Q5JVT0	49,680.1	310	100	12	5.19	25	2.107
20	Calmodulin, chain A	1CDLA	16,069.5	77	99.724	3	4.06	45	2.107
21	T-cell receptor V-alpha 12	S40138	13,028.4	64	94.231	4	4.79	31	2.1
nSCC									nSCC/SCC
22	Heat shock 27 kDa protein 1	Q96EI7	22,811.5	167	100	6	5.98	27	1.28
22	Hypothetical protein (fragment) (belongs to small HSP family)	Q96C20	21,185.6	156	100	7	5.55	40	1.283
23	Myosin-9 (myosin heavy chain, nonmuscle IIa)	MYH9	227,515	83	99.92	27	5.5	17	1.282
23	Lamin A/C	Q5TCI8	55,842.6	187	100	10	6.55	16	1.282
23	Progerin (lamin A/C)—homo sapiens	Q6UYC3	69,492.4	178	100	10	6.22	21	1.283
24	Rhabdomyosarcoma antigen MU-RMS-40.12	Q3BDU5	55,604.8	80	99.852	7	6.24	16	1.289
25	Myosin regulatory light chainl	MOHULP	19,838.5	108	100	3	4.67	23	1.306
25	Glyceraldehyde-3-phosphate dehydrogenase	DEHUG3	36,201.5	163	100	8	8.57	26	1.306
25	Aging-associated gene 9 protein	Q2TSD0	36,197.5	156	100	7	8.57	15	1.31
25	Nephrocystin-6	Q1PSK5	290,891.5	96	99.996	30	5.75	16	1.313
26	Centrosomal protein Cep290	CE290	180,298.3	82	99.911	23	6.43	16	1.329
27	AX886624 NID	CAF00762	6,869.5	69	98.297	4	11.71	21	1.338
28	CALD1 protein (Fragment)	Q6P707	21,078.4	79	99.809	7	5.01	26	1.34
28	NAG22 protein—Homo sapiens (human)	Q9NYG1	56,485.6	74	99.367	8	5.73	11	1.341
29	Nebulin (fragment)	Q14215	350,061.9	61	87.379	22	9.14	21	1.344
29	Lamin A/C	Q5TCI8	55,842.6	187	100	10	6.55	16	1.344
30	Desmoyokin—human (fragments)	A45259	312,579.6	62	91.065	12	6.29	11	1.353
31	Hypothetical protein DKFZp434E0130	Q7L890	15,848.8	60	84.473	4	9.07	20	1.376
32	AX886624 NID	CAF00762	6,869.5	64	94.362	4	11.71	21	1.377
32	Enolase 1	Q53HR3	47,453.4	98	99.998	7	7.01	33	1.377
32	HSM805698 NID	CAD97642	47,405.5	98	99.998	7	7.57	22	1.377
32	Myosin-9 (myosin heavy chain, nonmuscle IIa)	MYH9	227,515	72	99.166	15	5.5	13	1.377
32	HS2PPHAE NID	CAA59331	47,421.4	70	98.551	6	7.01	16	1.382
33	EN01 protein (fragment)	Q9BT62	30,149.3	60	86.784	5	5.63	11	1.389
34	Vimentin	Q5JVT0	49,680.1	435	100	18	5.19	18	1.38
35	Vimentin	A25074	53,676.1	430	100	18	5.06	18	1.426
36	Synaptonemal complex protein 1	Q5VT04	114,748.4	66	96.275	11	5.78	21	1.459
37	VAV1 protein	Q96D37	93,129.4	62	91.467	8	6.19	19	1.47
38	Hypothetical protein HNRPA3	Q53RW7	39,798.7	72	99.166	4	9.1	14	1.525
39	AF237621 NID (keratin)	AAF60327	66,149	192	100	4	8.16	12	1.528
40	AX886624 NID	CAF00762	6,869.5	64	94.362	4	11.71	12	1.532
41	Lamin A/C	Q5TCI8	55,842.6	187	100	10	6.55	16	1.655
42	Glyceraldehyde-3-phosphate dehydrogenase	DEHUG3	36,201.5	163	100	8	8.57	23	1.65
42	Aging-associated gene 9 protein	Q2TSD0	36,197.5	156	100	7	8.57	34	1.71
43	Nephrocystin-6	Q1PSK5	290,891.5	96	99.996	30	5.75	16	1.862
43	Glyceraldehyde-3-phosphate dehydrogenase	DEHUG3	36,070.4	101	99.999	3	8.58	40	1.86
n/a	Annexin 1	P04083	38,918	129	100	9	6.57	11	1.894

TABLE II. (*Continued*)

ID # from Figure 2	Protein identification	Accession number	Protein molecular weight (Da)	MOWSE score (PS)	Protein Score confidence interval	No. of matched peptides	pI	Sequence coverage (%)	Fold changes
44	Annexin 2	LUHU36	38,807.1	112	100	4	7.57	23	2.11
44	Reticulocalbin-3 precursor	Q96D15	37,470	185	100	10	4.74	50	2.114
45	Clathrin, light polypeptide	Q53XZ1	23,704.4	116	100	3	4.45	20	2.344
46	AF151903 NID	AAD34140	44,142.9	63	93.222	7	7.1	11	2.856
46	Enolase (alpha-enolase)	Q96X30	47,350.4	102	100	9	6.99	33	2.93
46	Phosphopyruvate hydratase-beta	S06756	47,285.4	82	99.906	7	7.05	25	3.21
46	Non-muscle myosin heavy polypeptide 9	Q60FE2	227,646.1	78	99.776	18	5.5	11	3.2
47	Myosin-9 (myosin heavy chain, nonmuscle IIa)	Q86XU5	227,515	78	99.77	18	5.5	13	3.368
47	Pyruvate kinase isozymes M1/M2	P14618	58,470.2	151	100	10	7.96	25	3.53
47	Glyceraldehyde-3-phosphate dehydrogenase	P04406	36,070.4	135	100	5	8.58	26	3.59
47	PKM2 protein (fragment)	Q8WUW7	37,594.6	134	100	7	8.47	25	3.72
47	Aging-associated gene 9 protein	Q2TSD0	36,197.5	129	100	4	8.57	34	3.967
48	Alpha-enolase	Q96X30	47,350.4	102	100	9	6.99	33	3.98
48	HS2PPHAE NID	CAA59331	47,421.4	90	99.986	8	7.01	16	3.98
48	Phosphopyruvate hydratase-beta	S06756	47,285.4	82	99.906	7	7.05	25	3.99
48	Myosin-9 (myosin heavy chain, nonmuscle IIa)	MYH9	227,515	78	99.77	18	5.5	17	3.99

The location of identified proteins on proteome reference maps can be observed in Figure 2 using the numbers under ID# from Figure 2.

when SCC and nSCC cells were karyotyped (data not shown), which indicates a potential cell population (SCCs) for transplantation study. The protein expression profiles presented here is therefore a reflection of the cells at a higher passage number, and hence the predominant expression of proteins involved in maintaining cellular integrity.

In our previous work we have demonstrated the existence of different sub-populations within the bone marrow stromal cells by isolating and expanding single-cell clonal populations [Mareddy et al., 2007]. The present study is a logical extension of our previous work in order to determine if the varying proliferation rates and differentiation potentials, seen between the fast- and slow-growing clones, were due to the expression of specific proteins.

For this investigation the authors selected three SCC clones and three nSCC clones. To narrow down the variation from patient's factors, each BMSC sample contained one SCC and one nSCC clones respectively. All SCC or nSCC clones were pooled for protein extraction and subsequent proteomic analysis. This is because protein fractionation by two-dimensional liquid chromatography (2D-LC), while offering improvements over two-dimensional gel electrophoresis in protein identification, requires substantially more total protein. Therefore, the current proteome expression generated from the pooled samples only reflected the difference between SCC and nSCC clones, but could not show differences within the three SCC or nSCC clones. The result yielded over 170 protein identities in the 196 liquid fractions assessed, for the purpose of the manuscript only the most confident results were included. Our proteomic analysis highlighted protein map found to be differentially expressed between SCCs and nSCCs. Comparative UV protein peaks which showed a fold change between 2 and 5 from the 2D liquid chromatography analysis were selected for further MALDI-TOF/TOF-MS identification. Of particular interest was the expression differences of proteins related to cell cycle, cell morphology, metabolism and proliferation. An over expression of calcium-binding and actin-binding proteins, such as CAM and TM, was evident in the fast-growing SCCs, which is particularly interesting since CAM regulates apoptosis in many cell types by binding to the death receptor Fas and thus blocking the Fas-mediated apoptosis [Ahn et al., 2004]. In addition, Ca^{2+}/CAM (calcium bound calmodulin) is known to play a vital role in releasing the brakes

TABLE III. Proteins of Specific Interest With Differential Expression Between SCC and nSCC

Protein identification	Accession number	Protein molecular weight (kDa)	MOWSE score	No. of matched peptides	Sequence coverage (%)	pI	Fold change	Molecular class
Proteins with increased abundance in SCC clones							SCC/nSCC	
Calmodulin	P62144	16.83	104	4	45	4.09	2.15	Calcium binding
Tropomyosin alpha-4 chain	P67936	28.5	89	4	17	4.67	2.96	Cytoskeleton
Corticotropin-lipoptotin (fragment)	P68000	4.54	79	1	53	8.09	3.44	Pituitary hormone
Proteins with increased abundance in nSCC clones							nSCC/SCC	
Annexin 1	P04083	38.9	129	9	38	6.57	1.89	Calcium binding
Lamin A/C	Q5TCI8	55.8	187	10	26	6.55	2.05	Intermediate filament
Progerin	Q6UYC3	69.5	178	10	21	6.22	1.99	Intermediate filament
Caldesmon	Q6P707	64.2	86	10	26	6.66	2.12	Cytokinesis
Heat shock protein 27	Q69EI7	22.4	185	8	42	7.83	2.02	Chaperone
Glyceraldehyde-3-phosphate dehydrogenase	P04406	36.2	163	8	40	8.57	3.23	Glycolytic protein
Pyruvate kinase isozyme M1/M2	P14618	58.5	144	9	26	7.90	3.36	Glycolytic protein
Enolase	Q96X30	47.3	102	9	33	6.99	2.85	Glycolytic protein

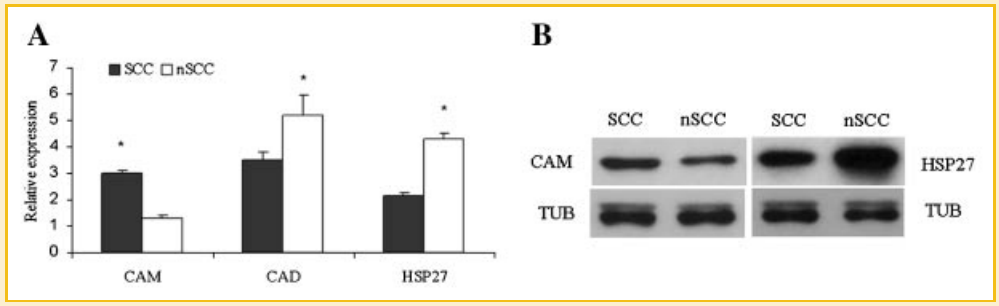

Fig. 3. Confirmation of the differential expression of proteins identified in the proteomic study. A: mRNA expression of calmodulin (CAM), caldesmon (CAD) and heat shock protein 27 (HSP27) was quantified by qRT-PCR. The figure shows the relative mRNA expression for each gene in comparison to the expression of the house keeping gene, 18S rRNA. CAM indicated up regulation in SCCs and CAD and HSP27 showed increased expression in nSCCs. B: Western blot analysis of CAM and HSP27 in SCCs and nSCCs. CAM was highly expressed in the SCCs compared with the expression in nSCCs, whereas HSP27 was expressed more in nSCCs The housekeeping gene alpha tubulin (TUB) was uniformly expressed in all the clones.

in CAD-regulated cytokinesis which affects the rate of cell division [Eppinga et al., 2006]. CAM also modulates osteoclastogenesis and therefore bone resorption during bone turnover [Zhang et al., 2003]. TM is reported to promote cytokinesis progression by stimulating the activation of actomyosin ATPase, which is required to accelerate cell division [Eppinga et al., 2006]. The potential over expression of CAM and TM in the fast-growing SCCs can be attributed to their role as modulators during cytokinesis and cell proliferation.

Corticotropin, a peptide hormone secreted by the pituitary gland, was another protein found to be over represented in the fast-growing SCCs. This hormone has a role in modulating the immune system by reducing the production of immunoglobulin by B-lymphocytes [Tsagarakis and Grossman, 1994]. Corticotropin treatment is reported to increase the proliferation of multipotential progenitor populations and also promote the development of a chondrocyte phenotype from multipotential progenitor populations [Evans et al., 2004]. Furthermore, corticotropin is known to stimulate keratinocyte proliferation thus playing a role in wound healing and also to activate the epithelial and mesenchymal cell proliferation and differentiation throughout the parenchyma during pulmonary maturation [Muglia et al., 1999].

Proteins found to be over expressed in slow-growing nSCCs included members of metabolic pathways, stress response and cytoskeletal proteins. Among these proteins, the role of CAD is of particular interest, since it binds to actin, myosin, and TM and inhibits TM-actin-activated myosin ATPase, establishing a regulated break to cytokinesis. TM and CAD are thought to play opposing roles in the regulation of actin-activated myosin during cytokinesis, and there appears to be a strong correlation between the state of myosin ATPase and rate of cell division [Eppinga et al., 2006]. Annexin-I (ANAX1) and annexin-2 were another two anti-proliferative proteins highlighted by our proteomics analysis, which

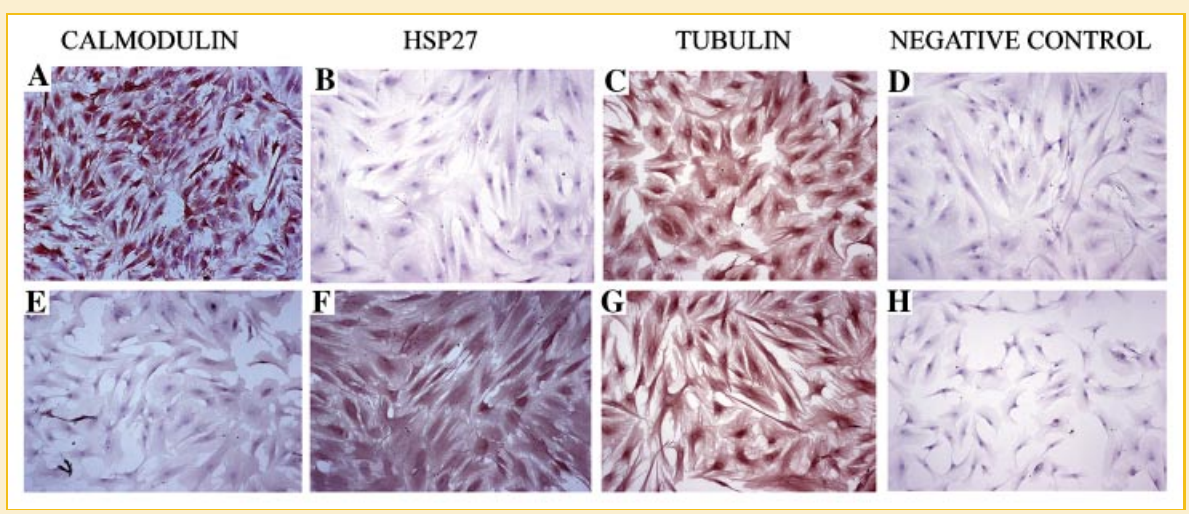

Fig. 4. Differential expression of CAM and HSP27 between the clonal populations as revealed by immunocytochemistry (10× magnification). For immunostaining cells were permeabilized and incubated with primary antibodies, CAM, HSP27, and TUB overnight. The upper panel (A–D) displays the results for SCCs which showed strong staining for CAM and weak staining for HSP27. Similarly, the lower panel (E–H) displays the differential expression of nSCCs which showed strong staining for HSP27 and weak staining for CAM. Both the clones uniformly expressed the protein for house keeping gene TUB. No staining was detected in the negative control (D and H). [Color figure can be viewed in the online issue, which is available at www.interscience.wiley.com.]

belong to the family of phospholipids and calcium-binding proteins associated with membrane, cytosol and cytoskeleton in a calcium-dependent manner. ANAX1 is reported to have a cell-type independent, anti-proliferative function through sustained activation of ERK (extracellular signal-regulated kinases) signaling cascade and by disruption of the actin cytoskeleton. Over expression of ANAX1 inhibits cyclin D1 expression affecting the normal cell morphology and therefore reducing the cell proliferation [Alldridge and Bryant, 2003]. Nuclear protein export is another important mechanism that regulates cell cycle transition. Nuclear retention of annexin II reduces cell proliferation and increases population doubling time. Expression of annexin II also causes morphological changes of the cells [Liu et al., 2003].

The elevated expression of proteins of the nuclear lamina, lamin A/C and progerin—the mutant form of lamin A—are also of high relevance to our study. Previous studies suggest that lamin A, and its C isoform, are predominantly expressed in differentiated cells and are dispensable during embryonic development, at least in the mouse [Gotzmann and Foisner, 2006; Mattout et al., 2006]. Furthermore, the expression of progerin in interphase cells is associated with lobulation of the nuclear envelope, thickening of the nuclear lamina and destabilization of cytokinesis, nuclear assembly and the cell cycle itself [Dechat et al., 2007]. HSP27, an ATP-independent chaperone that confers cytoprotection and the support of cell survival under stress conditions, was found to have an increased expression in the slow clones. In response to stress stimuli, expression and phosphorylation of HSP27 is increased [Rogalla et al., 1999] which in turn potentiates the degradation of ubiquinated proteins in vitro [Parcellier et al., 2003].

Besides the up-regulation of the cell cycle regulatory proteins mentioned above, metabolic pathway proteins, such as GAPDH and pyruvate kinase M2 (PKM2), were also found to have an increased expression. GAPDH is a glycolytic protein, which is pivotal in energy production, but which is now known to have other functions, seemingly independent of its role in glycolysis [Epner et al., 1999]. For example, GAPDH appears to play a critical role during apoptosis, in a variety of cell types, [Sunaga et al., 1995; Ishitani et al., 1996] by translocating to the nucleus, thereby acting as a signaling mechanism which activates transcription of pro-apoptic proteins. It has also been reported that nuclear translocation of PKM2 is sufficient to induce cell death that is independent of any caspase isoforms and enzymatic activity [Stetak et al., 2007]. Interestingly, observations have been made with regard to metabolic rate and its inverse proportionality to stem cell self-renewal [Sastry, 2004], which may possibly explain the abundant expression of the metabolic enzymes in slow-growing nSCCs; an indication of these cells reaching a Hayflick limit [Shay and Wright, 2000]. In a study employing autofluoresence spectroscopy it was revealed that cells with high metabolic activity had a corresponding high rate of cell differentiation, and low metabolic activity corresponded with self-renewal [Croce et al., 1999]. These techniques open up new alternative possibilities of separating out viable self-renewing cells in the absence of definitive cell surface molecular markers.

In conclusion, the protein profiling study of distinct cell populations, derived from the heterogeneous bone marrow stromal cells, has generated a proteome reference map of stem cell clones, which will provide valuable information for the understanding of stem cell self-renewal and differentiation. The identified proteins and their crosstalk appear to confer the altered status in which the cell populations exist. Of particular interest was the differential presentation of calmodulin, tropomyosin and caldesmon between SCCs and nSCCs. These proteins could be prospective molecular markers of different sub-populations found in bone marrow cells. Future studies will examine the functional properties of these molecules in MSC self-renewal and differentiation.

ACKNOWLEDGMENTS

The authors are grateful to Mr. Alun Jones at the Molecular and Cellular Proteomics Mass Spectrometry Facility, Australian Research Council Special Research Centre for Functional and Applied Genomics, the University of Queensland, for operating the MALDI-TOF/TOF-MS. Gratitude is also expressed to Ms. Navdeep Kaur for her assistance with western blot and to Mr. Thor Friis for his assistance with the real time-PCR.

REFERENCES

Ahn EY, Lim ST, Cook WJ, McDonald JM. 2004. Calmodulin binding to the Fas death domain. Regulation by Fas activation. J Biol Chem 279:5661–5666.

Alldridge LC, Bryant CE. 2003. Annexin 1 regulates cell proliferation by disruption of cell morphology and inhibition of cyclin D1 expression through sustained activation of the ERK1/2 MAPK signal. Exp Cell Res 290:93–107.

Banfi A, Muraglia A, Dozin B, Mastrogiacomo M, Cancedda R, Quarto R. 2000. Proliferation kinetics and differentiation potential of ex vivo expanded human bone marrow stromal cells: Implications for their use in cell therapy. Exp Hematol 28:707–715.

Betgovargez E, Knudson V, Simonian MH. 2005. Characterization of proteins in the human serum proteome. J Biomol Tech 16:306–310.

Blonder J, Xiao Z, Veenstra TD. 2006. Proteomic profiling of differentiating osteoblasts. Expert Rev Proteomics 3:483–496.

Croce AC, Spano A, Locatelli D, Barni S, Sciola L, Bottiroli G. 1999. Dependence of fibroblast autofluorescence properties on normal and transformed conditions. Role of the metabolic activity. Photochem Photobiol 69:364–374.

Dechat T, Shimi T, Adam SA, Rusinol AE, Andres DA, Spielmann HP, Sinensky MS, Goldman RD. 2007. Alterations in mitosis and cell cycle progression caused by a mutant lamin A known to accelerate human aging. Proc Natl Acad Sci USA 104:4955–4960.

Epner DE, Sawa A, Isaacs JT. 1999. Glyceraldehyde-3-phosphate dehydrogenase expression during apoptosis and proliferation of rat ventral prostate. Biol Reprod 61:687–691.

Eppinga RD, Li Y, Lin JL, Lin JJ. 2006. Tropomyosin and caldesmon regulate cytokinesis speed and membrane stability during cell division. Arch Biochem Biophys 456:161–174.

Evans JF, Niu QT, Canas JA, Shen CL, Aloia JF, Yeh JK. 2004. ACTH enhances chondrogenesis in multipotential progenitor cells and matrix production in chondrocytes. Bone 35:96–107.

Feldmann RE, Jr., Bieback K, Maurer MH, Kalenka A, Burgers HF, Gross B, Hunzinger C, Kluter H, Kuschinsky W, Eichler H. 2005. Stem cell proteomes: A profile of human mesenchymal stem cells derived from umbilical cord blood. Electrophoresis 26:2749–2758.

Foster LJ, Zeemann PA, Li C, Mann M, Jensen ON, Kassem M. 2005. Differential expression profiling of membrane proteins by quantitative proteomics in a human mesenchymal stem cell line undergoing osteoblast differentiation. Stem Cells 23:1367–1377.

Golan-Mashiach M, Dazard JE, Gerecht-Nir S, Amariglio N, Fisher T, Jacob-Hirsch J, Bielorai B, Osenberg S, Barad O, Getz G, Toren A, Rechavi G, Itskovitz-Eldor J, Domany E, Givol D. 2005. Design principle of gene expression used by human stem cells: Implication for pluripotency. FASEB J 19:147–149.

Gotzmann J, Foisner R. 2006. A-type lamin complexes and regenerative potential: A step towards understanding laminopathic diseases? Histochem Cell Biol 125:33–41.

Gronthos S, Zannettino AC, Hay SJ, Shi S, Graves SE, Kortesidis A, Simmons PJ. 2003. Molecular and cellular characterisation of highly purified stromal stem cells derived from human bone marrow. J Cell Sci 116: 1827–1835.

Hermansson M, Sawaji Y, Bolton M, Alexander S, Wallace A, Begum S, Wait R, Saklatvala J. 2004. Proteomic analysis of articular cartilage shows increased type II collagen synthesis in osteoarthritis and expression of inhibin betaA (activin A), a regulatory molecule for chondrocytes. J Biol Chem 279:43514–43521.

Ishitani R, Sunaga K, Hirano A, Saunders P, Katsube N, Chuang DM. 1996. Evidence that glyceraldehyde-3-phosphate dehydrogenase is involved in age-induced apoptosis in mature cerebellar neurons in culture. J Neurochem 66:928–935.

Kolf CM, Cho E, Tuan RS. 2007. Mesenchymal stromal cells. Biology of adult mesenchymal stem cells: Regulation of niche, self-renewal and differentiation. Arthritis Res Ther 9:204.

Lane CS. 2005. Mass spectrometry-based proteomics in the life sciences. Cell Mol Life Sci 62:848–869.

Liu J, Rothermund CA, Ayala-Sanmartin J, Vishwanatha JK. 2003. Nuclear annexin II negatively regulates growth of LNCaP cells and substitution of ser 11 and 25 to glu prevents nucleo-cytoplasmic shuttling of annexin II. BMC Biochem 4:10.

Mareddy S, Crawford R, Brooke G, Xiao Y. 2007. Clonal isolation and characterization of bone marrow stromal cells from patients with osteoarthritis. Tissue Eng 13:819–829.

Mattout A, Dechat T, Adam SA, Goldman RD, Gruenbaum Y. 2006. Nuclear lamins, diseases and aging. Curr Opin Cell Biol 18:335–341.

Muglia LJ, Bae DS, Brown TT, Vogt SK, Alvarez JG, Sunday ME, Majzoub JA. 1999. Proliferation and differentiation defects during lung development in corticotropin-releasing hormone-deficient mice. Am J Respir Cell Mol Biol 20:181–188.

Muraglia A, Cancedda R, Quarto R. 2000. Clonal mesenchymal progenitors from human bone marrow differentiate in vitro according to a hierarchical model. J Cell Sci 113(Pt 7): 1161–1166.

Panepucci RA, Siufi JL, Silva WA, Jr., Proto-Siquiera R, Neder L, Orellana M, Rocha V, Covas DT, Zago MA. 2004. Comparison of gene expression of umbilical cord vein and bone marrow-derived mesenchymal stem cells. Stem Cells 22:1263–1278.

Parcellier A, Schmitt E, Gurbuxani S, Seigneurin-Berny D, Pance A, Chantome A, Plenchette S, Khochbin S, Solary E, Garrido C. 2003. HSP27 is a ubiquitin-binding protein involved in I-kappaBalpha proteasomal degradation. Mol Cell Biol 23:5790–5802.

Park HW, Shin JS, Kim CW. 2007. Proteome of mesenchymal stem cells. Proteomics 7:2881–2894.

Phinney DG, Kopen G, Righter W, Webster S, Tremain N, Prockop DJ. 1999. Donor variation in the growth properties and osteogenic potential of human marrow stromal cells. J Cell Biochem 75:424–436.

Rogalla T, Ehrnsperger M, Preville X, Kotlyarov A, Lutsch G, Ducasse C, Paul C, Wieske M, Arrigo AP, Buchner J, Gaestel M. 1999. Regulation of Hsp27 oligomerization, chaperone function, and protective activity against oxidative stress/tumor necrosis factor alpha by phosphorylation. J Biol Chem 274:18947–18956.

Salasznyk RM, Westcott AM, Klees RF, Ward DF, Xiang Z, Vandenberg S, Bennett K, Plopper GE. 2005. Comparing the protein expression profiles of human mesenchymal stem cells and human osteoblasts using gene ontologies. Stem Cells Dev 14:354–366.

Sastry PS. 2004. Metabolic rate determines haematopoietic stem cell self-renewal. Med Hypotheses 63:476–480.

Shay JW, Wright WE. 2000. Hayflick, his limit, and cellular ageing. Nat Rev Mol Cell Biol 1:72–76.

Simmons PJ, Torok-Storb B. 1991. Identification of stromal cell precursors in human bone marrow by a novel monoclonal antibody, STRO-1. Blood 78:55–62.

Stetak A, Veress R, Ovadi J, Csermely P, Keri G, Ullrich A. 2007. Nuclear translocation of the tumor marker pyruvate kinase M2 induces programmed cell death. Cancer Res 67:1602–1608.

Sun HJ, Bahk YY, Choi YR, Shim JH, Han SH, Lee JW. 2006. A proteomic analysis during serial subculture and osteogenic differentiation of human mesenchymal stem cell. J Orthop Res 24:2059–2071.

Sunaga K, Takahashi H, Chuang DM, Ishitani R. 1995. Glyceraldehyde-3-phosphate dehydrogenase is over-expressed during apoptotic death of neuronal cultures and is recognized by a monoclonal antibody against amyloid plaques from Alzheimer's brain. Neurosci Lett 200:133–136.

Tsagarakis S, Grossman A. 1994. Corticotropin-releasing hormone: Interactions with the immune system. Neuroimmunomodulation 1:329–334.

Wang D, Park JS, Chu JS, Krakowski A, Luo K, Chen DJ, Li S. 2004. Proteomic profiling of bone marrow mesenchymal stem cells upon transforming growth factor beta1 stimulation. J Biol Chem 279:43725–43734.

Ye NS, Chen J, Luo GA, Zhang RL, Zhao YF, Wang YM. 2006. Proteomic profiling of rat bone marrow mesenchymal stem cells induced by 5-azacytidine. Stem Cells Dev 15:665–676.

Zhang L, Feng X, McDonald JM. 2003. The role of calmodulin in the regulation of osteoclastogenesis. Endocrinology 144:4536–4543.